© Indian Academy of Sciences

REGULAR ARTICLE

A new rhodamine based 'turn-on' Cu²⁺ ion selective chemosensor in aqueous system applicable in bioimaging

ABHISHEK MAJI, SOMENATH LOHAR, SIDDHARTHA PAL and
PABITRA CHATTOPADHYAY*

Department of Chemistry, The University of Burdwan, Golapbag, Burdwan, West Bengal 713 104, India
E-mail: pabitracc@yahoo.com

Abstract. A new rhodamine-based Schiff base (**L**) has been synthesized and characterized by physicochemical and spectroscopic tools. This organic molecule selectively reacts with Cu²⁺ ions with a remarkably significant optical change, which supports the development of a chemosensor for Cu²⁺ ions as low as nanomolar level in aqueous medium. On the basis of the experimental work, the '*turn-on*' colorimetric/fluorimetric spectroscopic change is due to Cu²⁺ ion-assisted hydrolysis followed by spirolactam ring opening of the probe (**L**) in 20 mM HEPES buffer [pH 7.4; water/acetonitrile (9:1 v/v)]. The competitive ions do not affect the selectivity and specificity of the probe (**L**) in the detection of Cu²⁺ ions. The cell imaging study using fluorescence microscope showed that this non-cytotoxic probe is useful to detect the distribution of Cu²⁺ ions in AGS cells lines.

Keywords. Hydrolysis; Cu²⁺ ions; rhodamine-B; cell imaging.

1. Introduction

A chemosensor is such a compound that exhibits a very distinguishable and a significant change in electrical, electronic, magnetic, or optical signal when it binds to a specific guest counterpart like cations, anions or molecules, *etc*.[1] As the third most abundant transition metal ion, Cu²⁺ (after Fe²⁺ and Zn²⁺) plays a pivotal role in a variety of fundamental physiological processes in organisms ranging from bacteria to mammals involving cellular energy generation, oxygen transport and activation, and signal transduction.[2–4] In many metalloenzymes, including superoxide dismutase, cytochrome c oxidase, and tyrosinase copper ion plays a crucial role as a catalytic cofactor.[5] Due to its widespread use, Cu²⁺ ion is also a significant metal pollutant in the environment.[6] Though Cu²⁺ plays important role in many biochemical processes, alteration in the cellular homeostasis of copper ions was reported to be connected with some serious neurodegenerative diseases like Alzheimer's disease,[7] Indian childhood cirrhosis (ICC),[8] Indian prion disease,[9] and Menkes and Wilson diseases.[10,11] A high amount of copper for a short period of time can also lead to gastrointestinal disturbance, liver or kidney damage.[12] Free copper ions in a live cell catalyze the formation of reactive oxygen species (ROS) that can damage lipids, nucleic acids, and proteins. As a result, the maximum permissible level of copper in drinking water has been set at 1.3 ppm ($\sim 20\,\mu$M) by the U.S. Environmental Protection Agency (EPA).[13]

Though, numerous methods for the detection of trace level of copper in the samples are available which include electrochemistry,[14] atomic absorption spectrometry,[15] inductively coupled plasma mass spectroscopy (ICPMS),[16] inductively coupled plasma atomic emission spectrometry (ICP-AES)[17] and voltammetry.[18] But these techniques are usually complicated, time-consuming and costly too.

Of the many different kinds of optical sensors, fluorescent chemosensors have several advantages over the other methods due to their intrinsic sensitivity, upfront application to fiber optical-based detection, and real-time monitoring with fast response time.[19,20] Due to its intrinsic paramagnetic properties, Cu²⁺ ion has the propensity to quench the fluorescence of fluorescent

---

*For correspondence

metal chelators conferring a non-fluorescent state.[21,22] In addition, most of the copper-selective sensors suffer from the interfering effect of cations such as Ni^{2+}, Ag^+, Hg^{2+} ions, *etc*.[23–26] Therefore, the development of a highly sensitive, selective *turn-on* fluorogenic probe working under a physiological condition with a fast response is highly desirable.

Rhodamine derivatives are non-fluorescent and colorless, whereas ring-opening of the corresponding spirolactam gives rise to strong fluorescence emission and a pink color. Several photosensing processes *viz.*, photo-induced electron transfer (PET),[27] photo-induced charge transfer (PCT),[28] fluorescence resonance energy transfer (FRET),[29] intermolecular charge transfer (ICT),[30] chelation enhanced fluorescence (CHEF),[31] *etc.*, are well known. Some hydroxynapthylidine derivatives and calixarene functionalised nanoparticles have been reported as Cu^{2+} ions sensor.[32,33] Rhodamine and its derivatives have been widely used to design fluorescent chemosensors due to their good photostability, high extinction coefficient, high fluorescence quantum yield and broad fluorescence in the visible region of electromagnetic spectrum. Several rhodamine-based chemosensors for recognition of various metal ions are reported.[34–39] With these considerations, herein, we report synthesis of a *salicylaldehyde* appended *rhodamine hydrazone* derivative (**L**) for selective determination of Cu^{2+} ions at physiological condition without interfering. Experimental findings suggest Cu^{2+} ions assisted spirolactam ring opening of (**L**) and the subsequent hydrolysis is responsible for fluorescence enhancement leading to *off-on* sensing.

2. Experimental

2.1 *Materials and general methods*

2.1a *Materials*:   High-purity HEPES buffer and rhodamine B dye were purchased from Himedia Laboratories, India. *3,5-Di-tert-butyl-2-hydroxybenzaldehyde* was purchased from Sigma Aldrich and different inorganic salts were purchased from Emplura, Merck. Analytical grade different solvents were purchased from commercial sources and they were used in this work without further purification (if not mentioned). Here, Milli-Q 18 Ω water was used throughout the experiments. UV-Vis and IR spectral data were collected using a Shimadzu (model UV-1800) spectrophotometer and a Prestige-21 SHIMADZU FTIR spectrometer, respectively. A Bruker Avance DPX 500 MHz spectrometer ^{1}H NMR spectra were recorded in DMSO-d_6. pH value of solution was adjusted using either 50 mM HCl or NaOH solution and the pH values were measured by using a Systronics digital pH

meter (model 335). A Thermochem Exactive plus mass spectrometer was used to get the electrospray ionization mass spectra. Steady state fluorescence emission and excitation spectra were obtained with the help of a Hitachi-7000 spectrofluorimeter.

2.1b *General methods*:   The fluorescence properties of the probe **L** were measured in 10% CH_3CN 20 mM HEPES buffer medium (pH 7.4) at 25 °C. To investigate the effect of different pH on the emission intensity of **L**, pH study was performed in 20 mM HEPES buffer solution by maintaining the pH using 50 mM HCl or 50 mM NaOH solution. Cell imaging study was carried out at biological pH ∼ 7.4 using 20 mM HEPES buffer solution. To check the selectivity of this probe **L** towards different metal ions, stock solutions ($\sim 10^{-2}$ M) for **L** was prepared using different salts: such as, the chloride salts of Ni^{2+}, Co^{2+}, Cu^{2+}, Au^{3+}, Hg^{2+}, Ca^{2+}, Mg^{2+} and Fe^{3+} ions; nitrate salts of Na^+, K^+, Cr^{3+} and Ag^+ ions; acetate salts of Mn^{2+} and Zn^{2+} ions; and ferrous sulphate in 10% CH_3CN 20 mM HEPES buffer (pH 7.4) solvent. During this selectivity measurement, the concentration of these metal ions was taken fifty times greater than that of the probe (**L**). For fluorimetric titration study, solution of copper(II) chloride dihydrate in 10% CH_3CN 20 mM HEPES buffer (pH 7.4) was used. During this study, probe concentration was 20.0 μM and gradually Cu^{2+} solution were added by varying Cu^{2+} concentration from 0 to 60.0 μM and the corresponding spectra were recorded.

The path length of the cells used for absorption and emission studies was 1 cm. For UV-Visible and fluorescence titrations, a stock solution of **L** was prepared in 10% CH_3CN 20 mM HEPES buffer (pH 7.4) at room temperature. Working solutions of **L** and Cu^{2+} ions were prepared from their respective stock solutions. Fluorescence measurements were performed using a 5 nm × 5 nm slit setting for both excitation and emission spectra. All the fluorescence and absorbance spectra were taken after 20 min of mixing the Cu^{2+} ions and **L**. A series of solutions containing **L** and $CuCl_2.2H_2O$ were prepared such that the total concentration of **L** (20 mM) remained constant in all the sets. The organic molecule (**L**) shows a very weak emission at 572 nm in 10% CH_3CN 20 mM HEPES buffer (pH 7.4) at 25 °C when excited at 550 nm.

2.2 *Synthesis of the probe (*L*)*

The probe **L** was synthesised by a two step reaction (Scheme 1). At first, the rhodamine B-hydrazide was prepared following a literature method.[40] In brief, 85% hydrazine hydrate (4 mL) was added to a solution of rhodamine B (1.0 g, 2.1 mmol) in ethanol (40 mL). The solution was refluxed for 6 h. Then, the reaction mixture was evaporated under reduced pressure to give an orange coloured oil, which was then recrystallized from methanol-water to afford rhodamine B-hydrazide as a light-orange crystal (77%).

In the second step, 3,5-Di-tert-butyl-2-hydroxybenzaldehyde (234.33 mg, 1.0 mmol) dissolved in ethanol was added to the ethanolic solution of rhodamine-B hydrazide (456.25
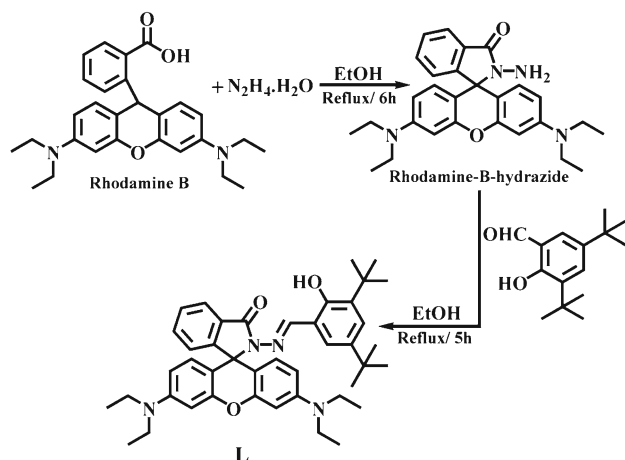
Scheme 1. Synthetic procedure of the probe (**L**)

mg, 1 mmol) with stirring. The resulting mixture was refluxed for 6 h. It was then evaporated to a small volume and cooled, from which white colored precipitate was filtered. The pure product was isolated from acetonitrile/methanol (3:1) mixed solvents on slow evaporation.

$C_{43}H_{52}N_4O_3$: M.p.: >250 °C. HRMS in methanol: [M + H]⁺, m/z, 673.3369 (100%) (calcd: m/z, 673.4118), where M = molecular weight of **L** (Figure S1), ^{1}H NMR (400 MHz, DMSO-d6): 11.18 (s, 1H); 8.85 (s, 1H); 7.94 (d, 1H); 7.61–7.66 (m, 2H); 6.956 (s.1 H); 6.36–6.45 (m.7H); 2.079 (s, 4H); 1.049–1.248 (m, 33H) (Figure S2), FT-IR (KBr, cm⁻¹): ν_{C-H}(aromatic), 2960.63; $\nu_{C=O}$, 1691.05; $\nu_{CH=N}$, 1614.39; $\nu_{C=C}$, 1514.51; ν_{C-N}, 1302.23; ν_{C-O-C}, 1118.64; ν_{C-H}(bending), 788.15 (Figure S3). Yield: 78%.

2.3 *Preparation of cell and in vitro cellular imaging with* **L**

Maintenance of the AGS cell lines used in this study was done in Dulbecco's modified eagle's medium (DMEM), supplemented with 10% fetal bovine serum (FBS), 2 mM glutamax, 100 μg.mL⁻¹ of penicillin and 100 μg.mL⁻¹ of streptomycin at 37 °C in a humidified incubator having 5% CO₂. The cultures were grown as monolayer and accepted once in 4–5 days by trypsinizing with 0.25% Trypsin-EDTA. AGS cells (4 x 10⁴ cells/mm²), plated on cover slips, were incubated with **L** (2, 5 and 10 μM, 1% DMSO) for 30 min. After washing with 50 mM phosphate buffer of pH 7.4 containing 150 mM NaCl (PBS), required volumes of copper(II) chloride solution in DMSO were added such that the final concentration of copper(II) chloride adjusted to 10.0 μM and 20.0 μM (DMSO will be 1%) and incubated for 30 min. The cells were fixed with 4% paraformaldehyde for 10 min at room temperature (RT). After washing with PBS, cover slips were mounted in 90% glycerol solution containing Mowiol (as an anti-fade reagent) and sealed. Images were acquired using Apotome fluorescence microscope (Carl Zeiss, Germany) using an oil immersion lens at 63X magnification. The images were analyzed using the AxioVision Rel 4.8.2 (Carl Zeiss, Germany) software.[41]

2.4 *Cell cytotoxicity assay*

To verify the usefulness of this probe in the biological system, the cytotoxicity of **L** was checked through MTT [*3-(4,5-dimethyl-thiazol-2-yl)-2,5-diphenyl tetrazolium bromide*] assay experiment[42] To the respective probe (5, 10, 25, 50, and 100 μM) solutions, 10 μL of MTT solution (10 mg/mL PBS) was added to each well of a 96-well culture plate and incubated continuously at 37 °C for 8 h. All the mediums were replaced with 100 μL of acidic isopropanol in the wells. The intracellular formazan crystals (blue-violet) formed were solubilized with 0.04 N acidic isopropanol and the absorbance of the solution was measured at 550 nm with a microplate reader. Absorbance values were recorded as the mean ± S.D. of three independent experiments.

3. Results and Discussion

3.1 *Synthesis and characterization*

The rhodamine B-hydrazide derivative probe (**L**) was prepared from the reaction 3,5-Di-tert-butyl-2-hydroxybenzaldehyde (TBHB) and rhodamine B-hydrazide in ethanol (Scheme 1). The crude white precipitate obtained from the reaction mixture was purified through crystallisation from the solution of **L** in acetonitrile/methanol (3:1) mixed solvents on slow evaporation over a few days. The crystallised product was characterized by physicochemical and spectroscopic tools (Figures S1–S3, in Supplementary Information).

### 3.2 *Absorption and fluorescence spectroscopic studies of* **L**

The UV-Visible spectra of **L** recorded in 10% CH₃CN 20 mM HEPES buffer (pH 7.4) at 25 °C shows an absorption maximum at 314 nm, which may be attributed to the intramolecular π–π* charge transfer transition.

On the stepwise addition of Cu²⁺ ions (0–60 μM) to the solution of **L** in 10% CH₃CN 20 mM HEPES buffer (pH 7.4), the absorption intensity at 314 nm increased gradually and a new peak at 560 nm was generated by ring opening with a visual color change from colorless to pink (Figure 1). In the presence of an excess of the biologically relevant transition metal ions (Cr³⁺, Mn²⁺, Fe³⁺, Co²⁺, Ni²⁺, Zn²⁺, Cd²⁺), alkali metal ions (Na⁺, K⁺), alkaline earth metal ions (Ca²⁺, Mg²⁺, Al³⁺) and other heavy metal ions (Hg²⁺, Pb²⁺), no new band was produced as they were unable to go through the ring opening step.

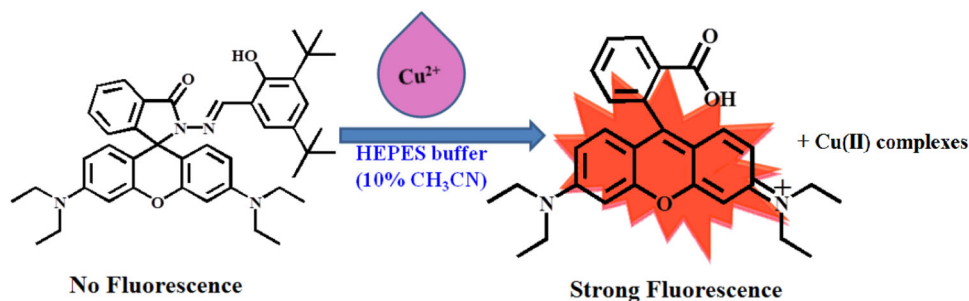The emission spectrum of **L** excited at 550 nm shows a fluorescence maximum at 572 nm in 10% CH₃CN
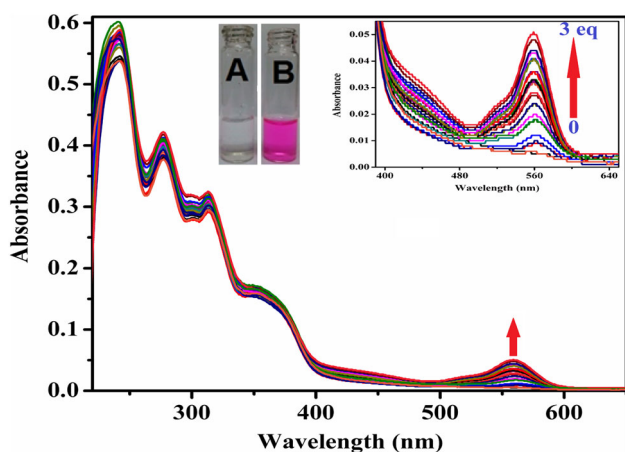
Figure 1. UV-Vis titration spectra of **L** (20 μM) upon gradual addition of Cu^{2+} ions (0–60 μM) in 10% CH_3CN 20 mM HEPES buffer (pH 7.4). [Inset] Visual color change of **L** (A) and **L** in presence of Cu^{2+} ions (B).
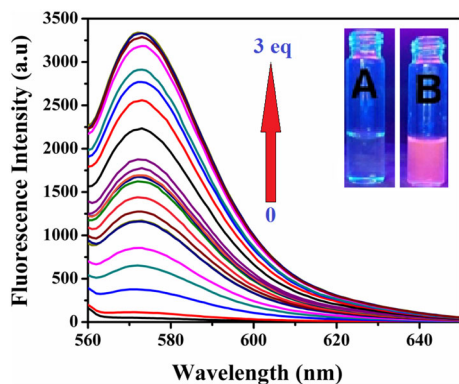
Figure 2. Emission spectra of **L** (20 μM) in presence of Cu^{2+} ions (0–60 μM) ($\lambda_{em} = 572$ nm, at $\lambda_{ex} = 550$ nm). Inset: Naked eye fluorescence color change: **(A)** **L** only, and **(B)** **L** in presence of Cu^{2+} ions in 10% CH_3CN 20 mM HEPES buffer (pH 7.4) at 25 °C.

20 mM HEPES buffer (pH 7.4) at 25 °C. When various concentrations of Cu^{2+} ions (0–60 μM) were added fluorescence intensity increases with an increase in the concentration of Cu^{2+} ions (Figure 2).

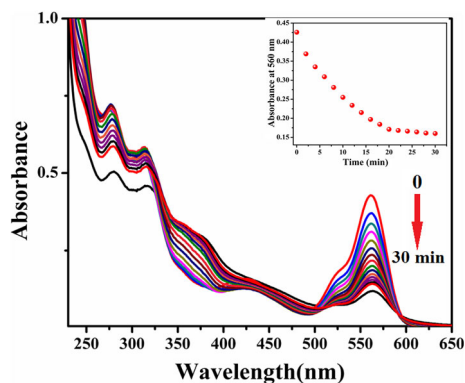**L** showed an almost 68-fold increase in its fluorescence intensity with the addition of only 3.0 equivalents of Cu^{2+} ions. This consequential strong fluorescence emission is due to the ring-opening of the spirolactam system of rhodamine-B (Scheme 2). In addition, this visual and fluorescence color change due to Cu^{2+} ions were not perturbed by the presence of an excess of the biologically relevance transition (Cr^{3+}, Mn^{2+}, Fe^{3+}, Co^{2+}, Ni^{2+}, Zn^{2+}, Cd^{2+}), alkali, alkaline earth metal ions (Na^+, K^+, Ca^{2+}, Mg^{2+}, Al^{3+}) and other heavy metal ions (Hg^{2+}, Pb^{2+}) (Figure S4 in SI) and also these ions did not offer such visual and fluorescent color change property through ring opening. It reveals that the probe **L** has an excellent selectivity and specificity towards Cu^{2+} ions over the other cations.

3.3 *pH study*

The effect of pH on the emission characteristics of **L** has been examined. Different sets of an equimolar mixture of **L** and Cu^{2+} ions were adjusted to different pH (pH 4.0–11.0) and their emission intensities were measured (*viz.*, Figure 3). This study clearly showed the maximum emission intensity of the [Cu^{2+} + **L**] system at pH 7.4,
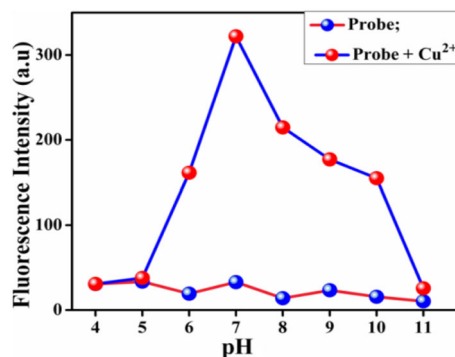
Figure 3. Effect of pH on the emission intensity of free **L** (20 μM) and [Cu^{2+} and **L**] system in 10% CH_3CN 20 mM HEPES buffer (pH 7.4) ($\lambda_{ex} = 550$ nm, $\lambda_{em} = 572$ nm).

Scheme 2. Schematic representation of plausible mechanism of Cu^{2+} sensing.

Figure 4. UV-Vis spectra of **L** in presence of Cu²⁺ ions (1.0 equiv.) with increase in time. (**Inset**) Plot of Absorbance of **L** (at $\lambda_{max} = 560$ nm) in presence of Cu²⁺ ions *vs.* Time.

which is in support of estimation of Cu²⁺ ions in any matrix at physiological pH.

3.4 *Mechanism*

In the presence of Cu²⁺ ions, **L** undergoes hydrolysis leading to open ring rhodamine unit, evidenced by the mass spectra and IR spectra (Figures S5 and S6 in Supplementary Information) of the products obtained from the final mixture of the probe and the added 3.0 equivalents of Cu²⁺ ions. As a result of hydrolysis of the probe followed by the ring opening, the increase of the emission intensity was observed with increasing addition of Cu²⁺ ions (Figure 2). It may be due to more and more hydrolysis of **L** in this condition followed by the formation of copper(II) complex of the fragmented part, irreversibly (Figure S5 on SI). However, no colorimetric change or no fluorescence enhancement of **L** occurred in the presence of other ions but interestingly, changes in color/fluorescence was observed only in the presence of Cu²⁺ ions in similar condition. Based on the MS spectral analysis, it has also been observed that the selective Cu²⁺ ions-assisted hydrolysis has occurred and it is different from the previous reports.[43–45] The emission and absorption spectra of **L** in the presence of Cu²⁺ ions was measured for a time period of 30 min and it was found that after ∼20 min the emission and absorbance reach a saturation level (Figure 4 and Figure S7 in SI). From the above discussions, the plausible mechanistic pathway of selective sensing Cu²⁺ ions by the probe **L** is presented in Scheme 2.

3.5 *Analytical figure of merit*

To investigate the selectivity, representative ions such as Na⁺, K⁺, Ca²⁺, Mg²⁺, Cr³⁺, Mn²⁺, Fe²⁺, Fe³⁺, Co²⁺,
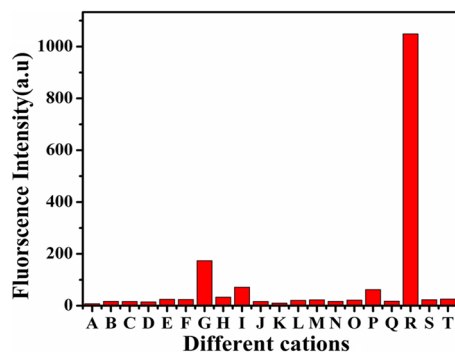
**Figure 5.** Fluorescence intensity of **L** in presence of different metal ions (at $\lambda_{em} = 572$ nm). (A) probe (**L**), (B) Co²⁺, (C) Mn²⁺, (D) Al³⁺, (E) Fe²⁺, (F) Mg²⁺, (G) Hg²⁺, (H) K⁺, (I) Pb²⁺, (J) Na⁺, (K) Fe³⁺, (L) Cd²⁺, (M) Cr³⁺, (N) Ba²⁺, (O) Ni²⁺, (P) Zn²⁺, (Q) Ca²⁺, (R) Cu²⁺, (S) Ag⁺, and (T) Au³⁺.
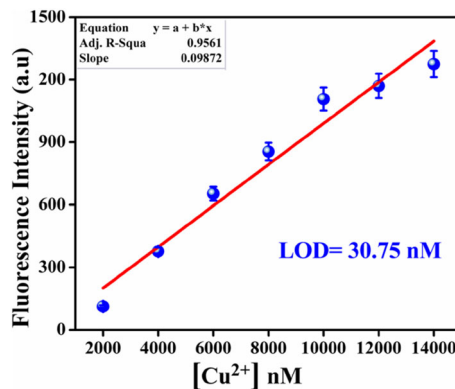
Figure 6. Calibration curve (with error bars) in the nanomolar range to calculate the LOD of Cu²⁺ ions using **L** from the fluorimetric titration data (at $\lambda_{em} = 572$ nm).

Ni²⁺, Cu²⁺, Zn²⁺, Cd²⁺, Hg²⁺, Pb²⁺, Ba²⁺, Sr²⁺, Ag⁺ and Au³⁺ ions were added to a solution of **L**, keeping the other experimental conditions unchanged. Only in the case of addition of Cu²⁺ ions a visible color change (colorless to pink) occurred along with an enhancement of fluorescence intensity. No significant change in the fluorescence intensity was observed with the addition of 10 equivalents (excess) of the above metal ions. Changes in the fluorescence spectra of **L** (20 μM) upon the addition of metal ions are also checked (Figure 5). This selectivity of Cu²⁺ ion over all other ions is due to the selective hydrolysis of **L**. From the linear response curve (Figure S8 in Supplementary Information), it is revealed that the probe exhibits a linearity with concentration of Cu²⁺ ions up to ∼ 46 μM.

The detection limit (LOD) was calculated from the calibration curve based on the fluorescence enhancement
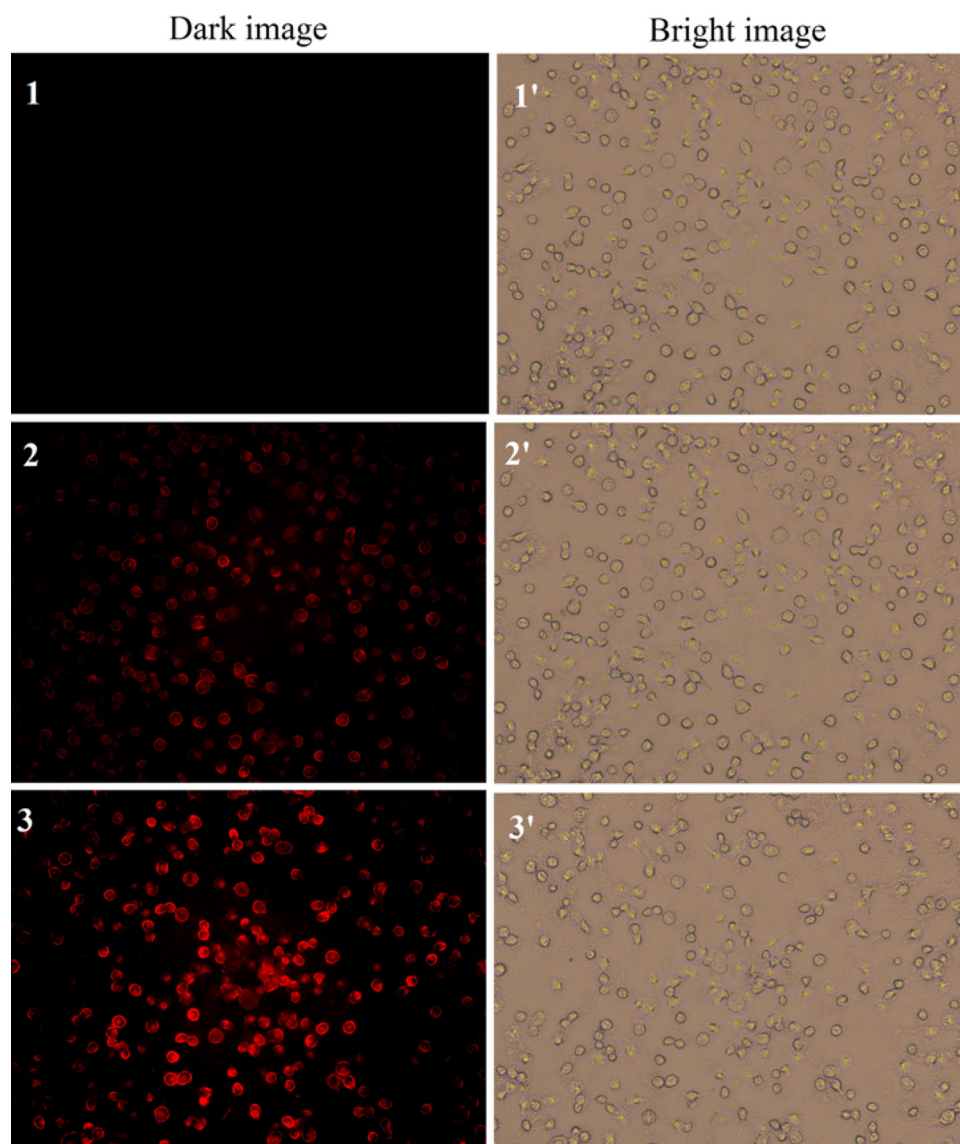
Figure 7. Fluorescence and bright field images of AGS cells after incubation with **L** (20 μM) followed by addition of Cu^{2+} ions, (1, 1') 0 μM, (2, 2') 10 μM and (3, 3') 20 μM, respectively. All the samples were excited at 550 nm by using a [63X] objective.

at 572 nm (Figure 6) by magnifying the lower concentration region of Cu^{2+} ions, using the equation $3\sigma/S$, where S is the slope of the line, and σ is the standard deviation of seven replicate measurements of the zero level.[46] LOD was found to be 30.75 nM. This indicates the efficiency of this probe towards the detection of Cu^{2+} ions in the nanomolar range.

3.6 *Application*

To investigate the utility of this probe (**L**) in biological systems, it was applied to AGS cell line. Here, **L** and Cu^{2+} were allowed to be taken up consecutively by the cells and the images of the cells were captured by fluorescence microscopy by excitation at $\sim$ 550 nm

(Figure 7). Additionally, *in vitro* study showed that the probe **L** is non-cytotoxic towards the cells up to 8.0 h (Figure S9 in SI). These results indicate that the probe has a huge potentiality for both *in vitro* and *in vivo* applications as a Cu^{2+} sensor as well as for live cell imaging.

4. Conclusions

A new fluorescence *turn-on* rhodamine-based Schiff base (**L**) has been synthesized and characterized by physicochemical and spectroscopic methods. The spectrophotometric color formation (colorless to reddish pink) and fluorimetric emission due to the selective Cu^{2+}

ion assisted hydrolysis, followed by spirolactam ring opening of the **L** in 10% CH$_3$CN 20 mM HEPES buffer (pH 7.4) at room temperature helps to detect Cu^{2+} ions as low as 30 nM in physiological condition. Interestingly, the presence of several competitive ions did not affect this color change. This non-toxic probe is also useful to identify the distribution of Cu^{2+} ions in living cells.

Supporting Information (SI)

Supplementary Information associated with this article is available at www.ias.ac.in/chemsci.

References

1. Jung H S, Kwon P S, Lee J W, Kim J-II, Hong C S, Kim J W, Yan S, Lee J Y, Lee J H, Joo T and Kim J S 2009 Coumarin-derived Cu^{2+}-selective fluorescence sensor: Synthesis, mechanisms, and applications in living cells *J. Am. Chem. Soc.* **131** 2008

2. Linder M C and Azam M H 1996 Copper biochemistry and molecular biology *Am. J. Clin. Nutr.* **63** 797S

3. Uauy R, Olivares M and Gonzalez M 1998 Essentiality of copper in humans *Am. J. Clin. Nutr.* **67** 952S

4. Gaggelli E, Kozlowski H, Valensin D and Valensin G 2006 Copper homeostasis and neurodegenerative disorders (Alzheimer's, Prion, and Parkinson's diseases and amyotrophic lateral sclerosis) *Chem. Rev.* **106** 1995

5. Zhou Y, Wang F, Kim Y, Kim S-J and Yoon J 2009 Cu^{2+}-selective ratiometric and "Off-On" sensor based on the rhodamine derivative bearing pyrene group *Org. Lett.* **11** 4442

6. Royzen M, Dai Z and Canary J W 2005 Ratiometric displacement approach to Cu(II) sensing by fluorescence *J. Am. Chem. Soc.* **127** 1612

7. Barnham K J, Masters C L and Bush A I 2004 Neurodegenerative diseases and oxidative stress *Nat. Rev. Drug Discovery* **3** 205

8. Hahn S H, Tanner M S, Danke D M and Gahl W A 1995 Normal metallothionein synthesis in fibroblasts obtained from children with indian childhood cirrhosis or copper-associated childhood cirrhosis *Biochem. Mol. Med.* **54** 142

9. Brown D R 2001 Copper and prion disease *Brain Res. Bull.* **55** 165

10. Waggoner D J, Bartnikas T B and Gitlin J D 1999 The role of copper in neurodegenerative disease *Neurobiol. Dis.* **6** 221

11. Vulpe C, Levinson B, Whitney S, Packman S and Gitschier J 1993 Isolation of a candidate gene for Menkes disease and evidence that it encodes a copper-transporting ATPase *Nat. Genet.* **3** 7

12. Sarkar S, Roy S, Sikdar A, Saha R N and Panja S S 2013 A pyrene-based simple but highly selective fluorescence sensor for Cu^{2+} ions *via* a *static* excimer mechanism *Analyst* **138** 7119

13. EPA US (1991) Maximum contaminant level goals and national primary drinking water regulations for lead and copper; final rule, Federal Register 56, 26460

14. Yang W, Jaramillo D, Gooding J J, Hibbert D B, Zhang R, Willett G D and Fisher K J 2001 Sub-ppt detection limits for copper ions with Gly-Gly-His modified electrodes *Chem. Commun.* **37** 1982

15. Becker J S, Matusch A, Depboylu C, Dobrowolska J and Zoriy M V 2007 Quantitative imaging of selenium, copper, and zinc in thin sections of biological tissues (Slugs-Genus Arion) measured by laser ablation inductively coupled plasma mass spectrometry *Anal. Chem.* **79** 6074

16. Becker J S, Zoriy M, Matusch A, Wu B, Salber D, Palm C and Becker J S 2010 Bioimaging of metals by laser ablation inductively coupled plasma mass spectrometry (LA-ICP-MS) *Mass Spectrom. Rev.* **29** 156

17. Ensafi A A, Khayamian T, Benvidi A and Mirmomtaz E 2006 Simultaneous determination of copper, lead and cadmium by cathodic adsorptive stripping voltammetry using artificial neural network *Anal. Chim. Acta* **561** 225

18. Zheng Y, Huo Q, Kele P, Andreopoulos F M, Pham S M and Leblanc R M 2001 A new fluorescent chemosensor for copper ions based on tripeptide glycyl-histidyl-lysine (GHK) *Org. Lett.* **3** 3277

19. Lai C Y, Trewyn B G, Jeftinija D M, Jeftinija K, Xu S, Jeftinija S and Lin V S Y 2003 A mesoporous silica nanosphere-based carrier system with chemically removable CdS nanoparticle caps for stimuli-responsive controlled release of neurotransmitters and drug molecules *J. Am. Chem. Soc.* **125** 4451

20. Shao N, Zhang Y, Cheung S, Yang R, Chan W, Mo T, Li K and Liu F 2005 Copper ion-selective fluorescent sensor based on the inner filter effect using a spiropyran derivative *Anal. Chem.* **77** 7294

21. Lim M H, Wong B A, Pitcock W H, Mokshagundam D, Baik M-H and Lippard S J 2006 Direct nitric oxide detection in aqueous solution by copper(II) fluorescein complexes *J. Am. Chem. Soc.* **128** 14364

22. Mondal B, Lohar S, Pal S, Maji A and Chattopadhyay P 2015 A new chemosensor selective for Cu^{2+} ions through fluorescence quenching approach applicable to real samples *J. Indian Chem. Soc.* **92** 1867

23. Mohammad R G, Tahereh P, Leila H B, Shohre R, Mohammad Y, Maryam R K, Abolghasem M, Hossein A and Mojtaba S 2001 Highly selective and sensitive copper(II) membrane coated graphite electrode based on a recently synthesized Schiff's base *Anal. Chim. Acta* **440** 81

24. Klein G, Kaufmann D, Schürch S and Reymond J-L 2001 A fluorescent metal sensor based on macrocyclic chelation *Chem. Commun.* **37** 561

25. Gatta's-Asfura K M and Leblanc R M 2003 Peptide-coated CdS quantum dots for the optical detection of copper(II) and silver(I) *Chem. Commun.* **39** 2684

26. Rurack K, Kollmannsberger M, Genger U R and Daub J 2000 A selective and sensitive fluoroionophore for Hg^{II}, Ag^{I}, and Cu^{II} with virtually decoupled fluorophore and receptor units *J. Am. Chem. Soc.* **122** 968

27. He G, Zhao X, Zhang X, Fan H, Wu S, Li H, He C and Duan C 2010 A turn-on PET fluorescence sensor for imaging Cu^{2+} in living cells *New J. Chem.* **34** 1055

28. Zhao H, Wang Y, Liu Z and Dai B 2014 Specific Cu(II) detection using a novel tricarbazolyl-tristriazolotriazine based on photoinduced charge transfer *RSC Adv.* **4** 13161

29. Pal S, Sen B, Mukherjee M, Dhara K, Zangrando E, Mandal S K, Khuda-Bukhsh A R and Chattopadhyay P 2014 Effect of substituents on FRET in rhodamine based chemosensors selective for Hg^{2+} ions *Analyst* **139** 1628

30. Xu Z, Xiao Y, Qian X, Cui J and Cui D 2005 Ratiometric and selective fluorescent sensor for Cu^{II} based on internal charge transfer (ICT) *Org. Lett.* **7** 889

31. Sen B, Mukherjee M, Banerjee S, Pal S and Chattopadhyay P 2015 A rhodamine-based 'turn-on' Al^{3+} ion-selective reporter and the resultant complex as a secondary sensor for F$^-$ ion are applicable to living cell staining *Dalton Trans.* **44** 8708

32. Dessingiou J, Khedkar J K and Rao C P 2014 Chemosensing ability of hydroxynaphthylidene derivatives of hydrazine towards Cu^{2+}: Experimental and computational studies *J. Chem. Sci.* **126** 1135

33. Gunupuru R, Maity D, Bhadu G R, Chakraborty A, Srivastava D N and Paul P 2014 Colorimetric detection of Cu^{2+} and Pb^{2+} ions using calix[4]arene functionalized gold nanoparticles *J. Chem. Sci.* **126** 627

34. Reddy U G, Ali F, Taye N, Chattopadhyay S and Das A 2015 A new turn on *Pd^{2+}*-specific fluorescence probe and its use as an imaging reagent for cellular uptake in Hct116 cells *Chem. Commun.* **51** 3649

35. Ali F, Saha S, Maity A, Taye N, Si M K, Suresh E, Ganguly B, Chattopadhyay S and Das A 2015 Specific Reagent for Cr(III): Imaging cellular uptake of Cr(III) in Hct116 cells and theoretical rationalization *J. Phys. Chem. B* **119** 13018

36. Mahato P, Saha S, Das P, Agarwalla H and Das A 2014 An overview of the recent developments on Hg^{2+} recognition *RSC Adv.* **4** 36140

37. Praveen L, Saha S, Jewrajka S K and Das A 2013 Self-assembly of modified rhodamine-6G with tri-block copolymer: unusual vesicle formation, pH sensing and dye release properties *J. Mater. Chem. B* **1** 1150

38. Mahato P, Saha S, Suresh E, Liddo R D, Parnigotto P P, Conconi M T, Kesharwani M K, Ganguly B and Das A 2012 Ratiometric detection of Cr^{3+} and Hg^{2+} by a naphthalimide-rhodamine based fluorescent probe *Inorg. Chem.* **51** 1769

39. Suresh M, Ghosh A and Das A 2008 A simple chemosensor for Hg^{2+} and Cu^{2+} that works as a molecular keypad lock *Chem. Commun.* 3906

40. Dujols V, Ford F and Czarnik A W 1997 A long-wavelength fluorescent chemodosimeter selective for Cu(II) ion in water *J. Am. Chem. Soc.* **119** 7386

41. McClintock J L and Ceresa B P 2010 Transforming growth factor-α enhances corneal epithelial cell migration by promoting EGFR recycling *Invest. Opthalmol. Vis. Sci.* **51** 3455

42. Banerjee S, Dixit A, Shridharan R N, Karande A A and Chakravarty A R 2014 *Endoplasmic reticulum* targeted chemotherapeutics: the remarkable photo-cytotoxicity of an oxovanadium(IV) vitamin-B6 complex in visible light *Chem. Commun.* **50** 5590

43. Wang S, Wang Z, Yin Y, Luo J and Kong L 2017 Coumarin-naphthol conjugated Schiff base as a "turn-on" fluorescent probe for Cu^{2+} via selective hydrolysis of imine and its application in live cell imaging *J. Photochem. Photobiol. A Chem.* **333** 213

44. Sahana S, Mishra G, Sivakumar S and Bharadwaj P K 2017 Highly sensitive and selective "turn-on" chemodosimeter based on Cu^{2+} - promoted hydrolysis for nanomolar detection of Cu^{2+} and its application in confocal cell imaging *J. Photochem. Photobiol. A Chem.* **334** 47

45. Wang L, Yan J, Qin W, Liu W and Wang R 2012 A new rhodamine-based single molecule multianalyte (Cu^{2+}, Hg^{2+}) sensor and its application in the biological system *Dyes Pigm.* **92** 1083

46. Pal S, Lohar S, Mukherjee M, Chattopadhyay P and Dhara K 2016 A fluorescent probe for the selective detection of creatinine in aqueous buffer applicable to human blood serum *Chem. Commun.* **52** 13706